Transactions of the Materials Research Society of Japan 32[3] 693-696 (2007)

Improvement of lithium secondary battery properties by blending $LiMn_2O_4$ nano particles with different composition

Izumi Mukoyama, Takashi Ogihara, Nobuo Ogata and Koji Nakane
Graduate School of Fiber Amenity Engineering, University of Fukui
3-9-1 Bunkyo, Fukui-shi, Fukui, 910-8507, Japan
Fax: 0776-27-8624, e-mail: ogihara@matse.fukui-u.ac.jp

The effect of blending $LiMn_2O_4$ nano particles with different composition was investigated to improve electrical properties of lithium secondary battery. As-prepared powders were synthesized by ultrasonic spray pyrolysis using metal nitrate solution. XRD showed that blended $LiMn_2O_4$ powders were well crystallized to a spinel structure with $Fd\bar{3}m$ space group. The blended particles have non-spherical morphology with an average diameter of about 0.5 μm in a diameter and a narrow size distribution. The charge/discharge capacity of blended $LiMn_2O_4$ exhibited stable cycle performance over 100 mAh/g at 0.5 mA/cm^2 between 3.5 and 4.4 V. The cycle performances of blended $LiMn_2O_4$ maintained about 90 mAh/g after 100th cycle at 80℃. Reduced Jahn-Teller distortion of lithium manganese by blending $LiMn_2O_4$ was the causes for enhanced cycle performance of $LiMn_2O_4$.

Keywords: Lithium manganese, Battery, Spray, Spinel, Jahn-Teller distortion

INTRODUCTION

Lithium cobalt oxide ($LiCoO_2$) and lithium nickel oxide ($LiNiO_2$) are promising compounds for use as a positive electrode material in lithium secondary batteries using a carbon negative electrode, because they show 4 V discharge voltage [1-5]. Cellular phone and notebook computer are used as power sources. However, $LiCoO_2$ and $LiNiO_2$ suffer the high cost of cobalt and toxicity. Lithium spinel manganese ($LiMn_2O_4$) and lithium transition metal oxide are the most attractively investigated cathode materials for lithium secondary batteries because of their three dimensional Li ion diffusion, low cost, high-natural abundance of manganese, and low toxicity [6-8]. Lithium ion secondary batteries are regarded as the future power sources for the hybrid-type electric vehicles (HEV) and zero emission vehicles (ZEV). Unfortunately, it has not proved successful to substitute $LiCoO_2$ with $LiMn_2O_4$ due to the degradation of its capacity on cycling. This is commonly considered to be due to dissolution of Mn: $2Mn^{3+} \rightarrow Mn^{4+}+Mn^{2+}$ [9]. The factor is that capacity fading is due to spinel dissolution [10], the Jahn-Teller distortion [11]. The spray pyrolysis preparation method for lithium ion battery cathode materials is an effective production technique for the rapid and increased powder production [12,13]. This method offers the following advantages: (i) the particles produced are spherical, (ii) the distribution of their diameters is uniform and controllable from micrometer to submicron, (iii) the purity of the product is high and (iv) the process is continuous. The smaller particles and good crystallinity will be bring out to overcome the fault of lithium manganese spinel. In this paper, the effect of blending $LiMn_2O_4$ nano particles with different composition was investigated to improve electrical properties of lithium secondary battery and particles such as crystallinity and morphology.

EXPERIMENTAL

$LiMn_2O_4$ precursor was used $LiNO_3$ and $Ni(NO_3)_2 \cdot 6H_2O$ as starting materials. $LiNO_3$ and $Ni(NO_3)_2 \cdot 6H_2O$ were dissolved in distilled water in the molar ratio of metal components (Li:Mn=1:2, Li:Mn=1:1 and Li:Mn=1.09:2) to prepared aqueous solutions with a total concentration of 0.5 mol/dm^3, respectively. As-prepared powders were synthesized from $LiMn_2O_4$ precursor by ultrasonic spray pyrolysis method. The starting solution was misted at a

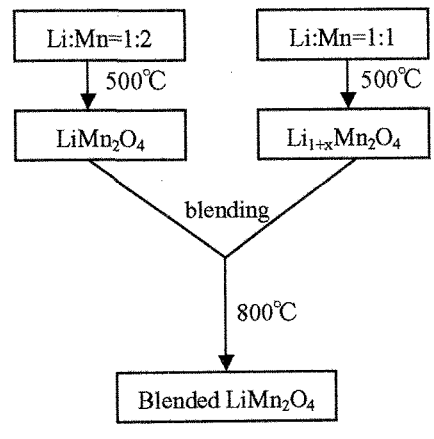

Fig.1. Synthesized process by blending $LiMn_2O_4$

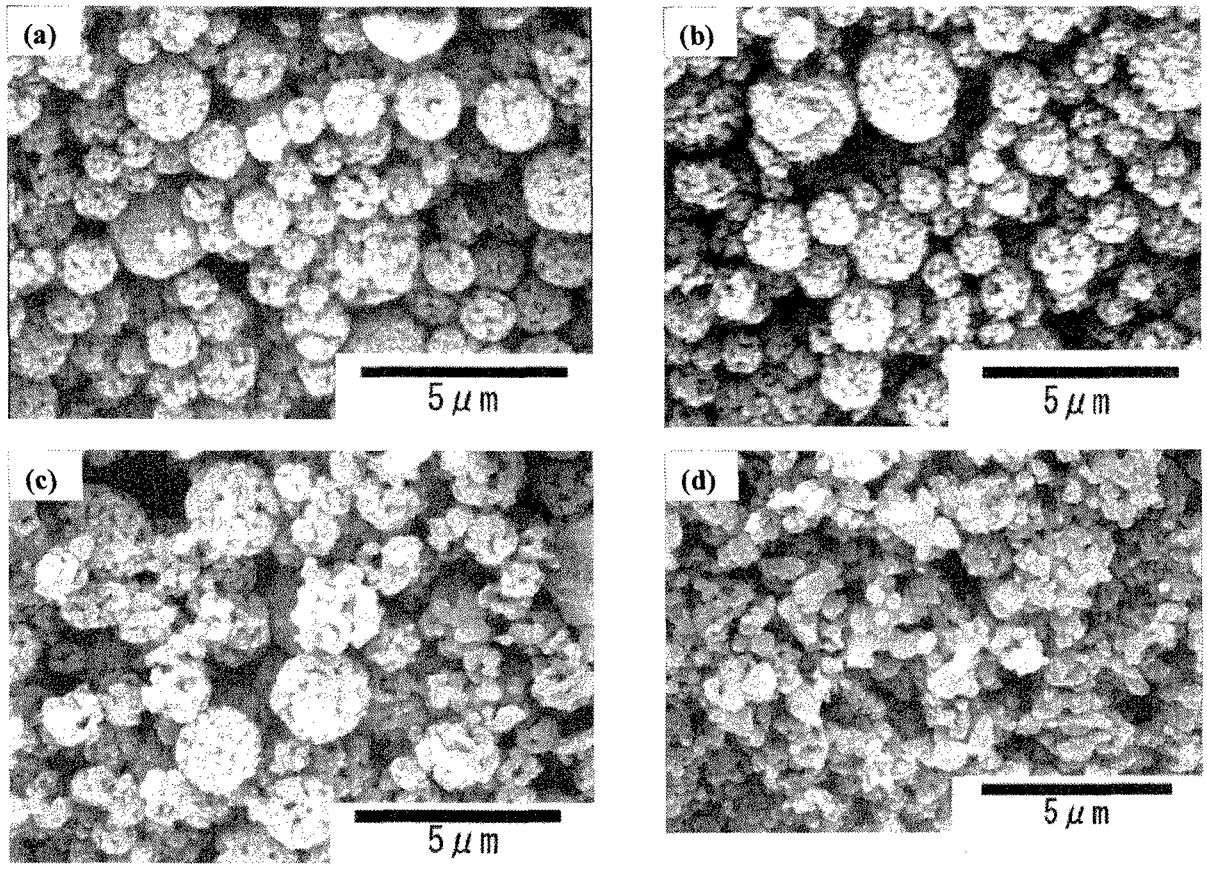

Fig.2. SEM photographs of (a)$LiMn_2O_4$, (b)$Li_{1+x}Mn_2O_4$, (c)$Li_{1.09}Mn_2O_4$ and (d)blended $LiMn_2O_4$

frequency of 2.4 MHz by an ultrasonic nebulizer (HM-2412, Honda Electronics). The average droplet size of the mist was about 3 μm in a diameter. The generated mist was carried to an electric furnace by air carrier gas with a rate of 0.7 dm^3/min and then pyrolyzed at 500℃. The scheme to synthesize blend $LiMn_2O_4$ is shown in Fig.1. Blended $LiMn_2O_4$ mixed $LiMn_2O_4$ and $Li_{1+x}Mn_2O_4$ (10:2 in weight) was calcined at 800℃ for 2h in air. The molar ratio of metal components of blended $LiMn_2O_4$ was Li:Mn=1.09:2. The crystalline structures of $LiMn_2O_4$, $Li_{1.09}Mn_2O_4$ and blended $LiMn_2O_4$ were characterized by X-ray diffraction (XRD, Shimadzu, XRD-6100). The surface morphology, microstructure and average particle size of $LiMn_2O_4$, $Li_{1.09}Mn_2O_4$ and blended $LiMn_2O_4$ were observed with a scanning electron microscope (SEM, Hitachi, S-2300). The average particle size was determined from measurement of particle diameter by randomly sampling of 300 particles from SEM photographs. The thermal decomposition behavior of the calcined powders was examined by means of thermogravimetric analysis and differential thermal analysis using a thermal analyzer system (DTA-TG, Shimadzu, DTA-TG-60) at a heating rate of 10℃/min in air. Electrochemical measurements were carried out using a two-electrode coin-type cell (CR2032) with lithium foil as the anode. The cathode slurry was composed of active materials (75wt.%), acetylene black powders (15wt.%) and polyvinylidene fluoride (PVdF, 10wt.%) in N-methyl-2-pyrrolidinone (NMP). The slurry was coated on an aluminum sheet, then dried at 120℃ for 24h in a vacuum oven. The electrolyte was 1 mol/dm^3 $LiPF_6$ in ethylene carbonate / diethyl carbonate (EC : DEC = 1 : 1) (Tomiyama Pure Chemical). Lithium battery was assembled in a glove box filled with argon gas. The cyclic voltammograms of $LiMn_2O_4$, $Li_{1.09}Mn_2O_4$ and blended $LiMn_2O_4$ were measured by potentiostat (Hokuto denko HSV-100) between 3.5 and 4.5 V at a sweep rate of 0.02 mV/s. The galvanostatic charge/discharge tests were measured in a voltage range between 3.5 and 4.4 V at different current densities on a battery tester (BTS-2004, Nagano).

RESULTS AND DISCUSSION

Figure 2 shows SEM photographs of $LiMn_2O_4$, $Li_{1.09}Mn_2O_4$ and blended $LiMn_2O_4$ powders calcined at 800℃ for 2h, respectively. $LiMn_2O_4$ and $Li_{1.09}Mn_2O_4$ powders had the spherical morphology with aggregation and consist of primary particles with about 10 – 100 nm, but blended $LiMn_2O_4$ showed the non-spherical morphology with higher crystallinity. The all particle size was showed in Table I . $LiMn_2O_4$ and $Li_{1.09}Mn_2O_4$

Table I Particle size of powders

Material	Particle size
$LiMn_2O_4$	1.32μm
$Li_{1+x}Mn_2O_4$	1.05μm
$Li_{1.09}Mn_2O_4$	1.21μm
Blended $LiMn_2O_4$	0.51μm

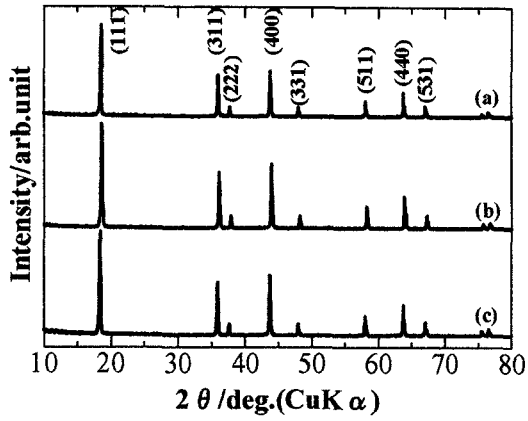

Fig.3. XRD patterns of (a)$LiMn_2O_4$, (b)$Li_{1.09}Mn_2O_4$ and (c) blended $LiMn_2O_4$

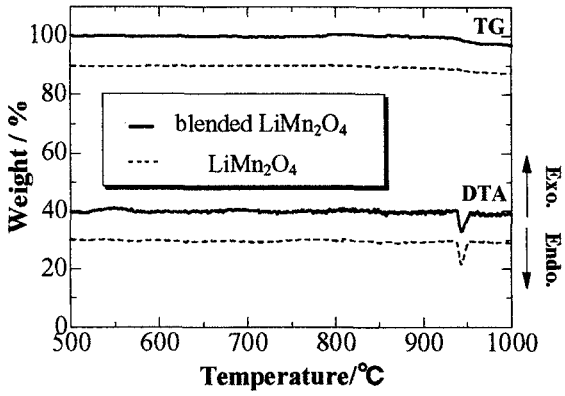

Fig.4. DTA-TG curvers of blended $LiMn_2O_4$ and $LiMn_2O_4$

powders were about 1.2 μm in a diameter, but blended $LiMn_2O_4$ powders was smaller particles (about 0.5 μm in a diameter). The values of geometrical standard deviation (σ_g) calculated from the particle size distribution of $LiMn_2O_4$, $Li_{1.09}Mn_2O_4$ and blended $LiMn_2O_4$ were 1.28, 1.34 and 1.37, respectively. Figure 3 shows the XRD patterns of blended $LiMn_2O_4$, $Li_{1.09}Mn_2O_4$ and $LiMn_2O_4$. All the powders were characterized the standard spinel structure with a space group of $Fd\bar{3}m$ in which the lithium ions occupy the tetrahedral (8a) sites and the manganese ions at the octahedral (16d) site. The diffraction lines of impurity peak (e.g. Mn_2O_3) except for spinel phase were not observed. Figure 4 shows DTA-TG between 500 and 1000℃ of $LiMn_2O_4$ and blended $LiMn_2O_4$. The TG curves of $LiMn_2O_4$ and blended $LiMn_2O_4$ decreased in mass dropping over 940℃. The DTA curves of $LiMn_2O_4$ and blended $LiMn_2O_4$ were observed endothermic peak with melting of powders. Figure 5 shows cyclic voltammograms (at 0.02 mV/s) of $LiMn_2O_4$, $Li_{1.09}Mn_2O_4$ and blended $LiMn_2O_4$. The well separated peaks in $LiMn_2O_4$ were found, but $Li_{1.09}Mn_2O_4$ has smaller separated peaks. Moreover, the peak of blended $LiMn_2O_4$ was observed only one. This result will give restraining dissolution of manganese ion. Figure 6 shows the discharge curves of $LiMn_2O_4$, $Li_{1.09}Mn_2O_4$ and blended $LiMn_2O_4$ between 3.5 and 4.4 V at 1 mA/cm^2, respectively. The discharge capacity of $LiMn_2O_4$ was 118mAh/g. The voltage jump was observed at 4.1 V in the discharge curve. The discharge capacity of $Li_{1.09}Mn_2O_4$ decreased 102 mAh/g due to addition of rich lithium ion. $Li_{1.09}Mn_2O_4$ had smaller voltage jump of discharge curve. The discharge capacity of blended $LiMn_2O_4$ was 101 mAh/g. However, S shape of discharge curve was obtained and clear voltage jump was disappeared at 4.1 V by blending $LiMn_2O_4$ nano particles with different composition. This finding suggested that the electrochemical reaction of lithium manganese during lithium insertion and extraction was a homogenous phase reaction. Therefore, this leads to the improvement of cycle performance of spinel lithium manganese. Figure 7 shows the change of discharge capacity as a function of cycle number at 0.5mA/cm^2 at room temperature. The discharge capacity of $LiMn_2O_4$ and $Li_{1.09}Mn_2O_4$ gradually decreased with increasing cycle number. On the other hand, the discharge capacity of blended $LiMn_2O_4$ was observed the stable cycle performance during 100 cycles. Improvement of lithium secondary battery properties by blending $LiMn_2O_4$ nano particles with different composition reduced Mn dissolution. Figure 8 shows the cycle performances of blended $LiMn_2O_4$ at various discharge rates. All three plots exhibited very stable cycle performance at the various discharge rates. This means that blending $LiMn_2O_4$ is effective for improving the high rate capability. Figure 9 shows the cycle performances of blended $LiMn_2O_4$ and $Li_{1.09}Mn_2O_4$ at 80℃. The discharge capacity retention of each powder was compared at high temperature. The discharge capacity of blended $LiMn_2O_4$ was higher than that of $Li_{1.09}Mn_2O_4$, maintained at about 90 mAh/g after 100th cycle at 0.5 mA/cm^2. Therefore,

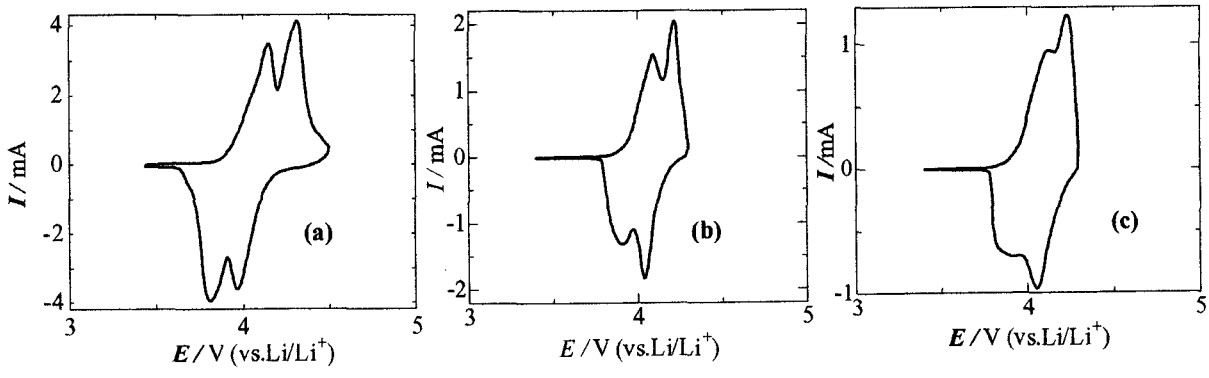

Fig.5. Cyclic voltammograms of (a)$LiMn_2O_4$, (b)$Li_{1.09}Mn_2O_4$ and (c)blended $LiMn_2O_4$

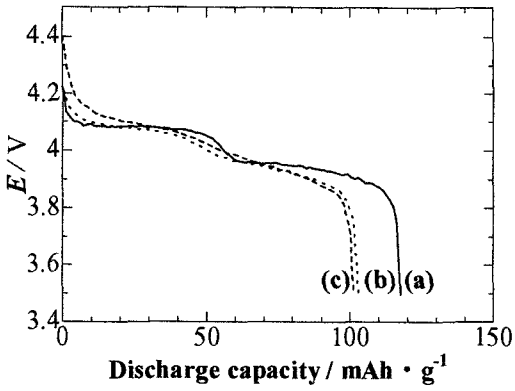

Fig.6. Discharge curves of (a)$LiMn_2O_4$, (b)$Li_{1.09}Mn_2O_4$ and (c)blended $LiMn_2O_4$

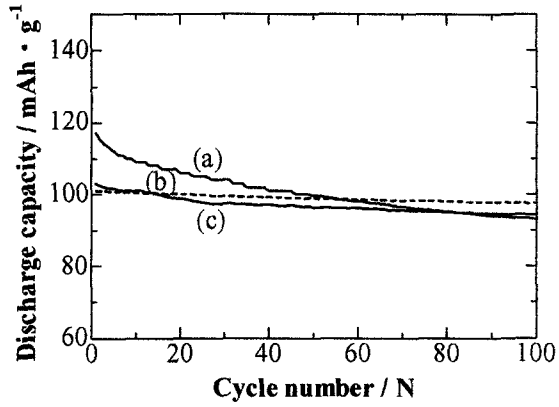

Fig.7. Cycle performances of (a)$LiMn_2O_4$, (b) blended $LiMn_2O_4$ and (c) $Li_{1.09}Mn_2O_4$

Blending $LiMn_2O_4$ nano particles with different composition reduced Mn dissolution in the high temperature.

CONCLUSION

Blending $LiMn_2O_4$ nano particles with different composition exhibited to improve electrical properties of lithium secondary battery. XRD of blended $LiMn_2O_4$ revealed were well crystallized to a spinel structure with $Fd\bar{3}m$ space group. The blended particles have non-spherical morphology with an average diameter of about 0.5 μm and a narrow size distribution. The charge/discharge capacity of blended $LiMn_2O_4$ exhibited stable cycle performance over 100mAh/g at 0.5 mA/cm^2. The blended $LiMn_2O_4$ powders showed good cycle performance at various discharge rates. The cycle performances of blended $LiMn_2O_4$ maintained about 90 mAh/g after 100th cycle at 80℃.

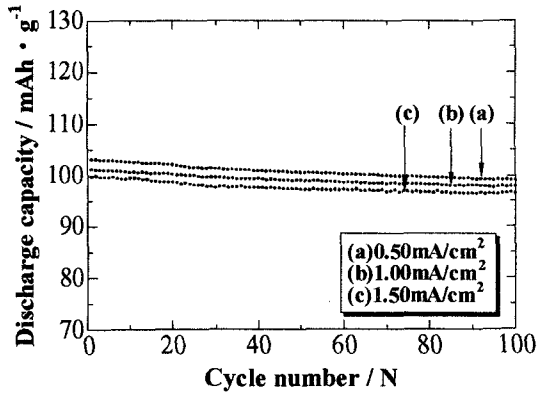

Fig.8. Cycle performances of blended $LiMn_2O_4$ at various discharge rates

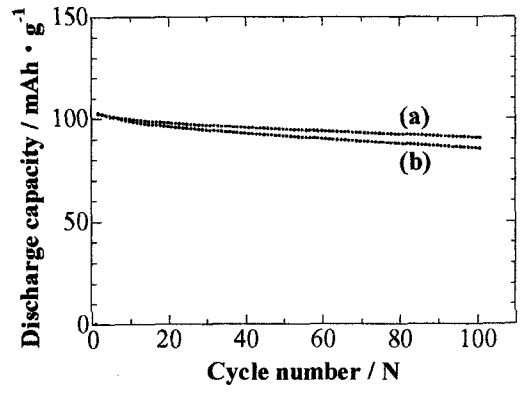

Fig.9. Cycle performances of (a)blended $LiMn_2O_4$ and (b)$Li_{1.09}Mn_2O_4$ at 80℃

ACKNOWLEDGEMENT

This work was supported by New Energy and Industrial Technology Development Organization.

REFERENCES

[1]K. Mizuhima, P. C. Jones, P. J.Wiseman, B.Goodenough, Mater.Res.Bull., **15**, 783 (1980).
[2]F. Capitaine, P. Gravereau, C. Delmas, Solid State Ionics., **69**, 59 (1994).
[3]J. M. Tarascon, d. Guyomard, Electrochim Acta., **38**, 1221 (1993).
[4]J. R. Dahn, U. von Sacken and C. A. Michel, Solid State Ionics., **44**, 87 (1990).
[5]T. Ohzuku, A. Ueda and M. Nagayama, J. Electrochem. Soc., **140**, 1862 (1993).
[6]T. Tsumura, A. Shimizu, M. Inagaki, J. Mater. Chem., **3**, 995 (1993).
[7]M. M. Thackeray, J. Electrochem. Soc., **142**, 2558 (1995).
[8]Y. Xia, Y. Zhou, M. Yoshio, J. Electrochem. Soc., **144**, 2593 (1997).
[9]Y. Xia, M. Yoshio, J. Power Soures., **66**, 129 (1997).
[10]D. H. Jang, J. Y. Shin, S. M. Oh, J. Electrochem. Soc., **143**, 2204 (1996).
[11]R. J. Gummow, A. de Kock, M. M. Thackerya, Solid State Ionics., **69**, 59 (1994).
[12]G. L. Messing, S. C. Zhang, G.V. Jayanthi, J. Am. Ceram. Soc., **76**, 2707 (1993).
[13]S. H. Park, S. K. Kang, Y. C. Kang, Y. S. Lee, Chem. Lett., **32**, 446 (2003).

(Received January 20, 2007;Accepted May 10, 2007)